Renewable Energy 206 (2023) 367–374

Contents lists available at ScienceDirect

Renewable Energy

journal homepage: www.elsevier.com/locate/renene

Linear uncertain modelling of LIDAR systems for robust wind turbine control design

Irene Miquelez-Madariaga [a,*], Idoia Lizarraga-Zubéldia [b], Asier Diaz de Corcuera [c], Jorge Elso [a]

[a] Department of Engineering, Public University of Navarre (UPNA), Campus de Arrosadia, 31006, Pamplona, Spain
[b] VORS CONTROL, Pamplona, Spain
[c] Siemens Gamesa Renewable Energy, Sarriguren, Spain

ARTICLE INFO

Keywords:
Light detection and ranging
Coherence
Wind turbine
Non parametric uncertainty

ABSTRACT

Light detection and ranging (LIDAR) sensors measure the free wind ahead of the rotor, enabling the use of new feedforward control strategies. However, there exist some sources of error inherent to the measuring process that should be considered during the design of LIDAR-based controllers. Typically, the coherence function is used for that purpose, but it is not compatible with some robust design methodologies. This paper presents an analytic relation between the coherence function and a non-parametric uncertainty model of LIDAR sensors, suitable for the design of controllers via μ-synthesis or Quantitative Feedback Theory. Such a relation is applied to a realistic LIDAR simulator. First, the linear non-parametric uncertainty model is identified using simulation data obtained from the well-known NREL 5 MW wind turbine. Then, it is validated against the coherence model by comparing linear predictions of the simulation outputs.

1. Introduction

Light detection and ranging (LIDAR) sensors provide a remote measurement of the wind ahead of the rotor of a wind turbine. As LIDAR measurements are less disturbed than the ones provided by traditional anemometry and have some preview, they open the door to feedforward control strategies. However, LIDAR sensors still present sources of error during the measurement process, such as information loss by sampling, that have an impact on the performance of LIDAR-based control. Consequently, a model of the measurement error should be considered during the controller design process [1].

There exist two main ways of dealing with the measurement error regarding the design of LIDAR-based controllers. The most common one is known as sequential design [2], and entails two independent steps. The first one consists on a processing stage in which the main objective is to make measured wind as similar as possible to the average wind speed in the rotor plane. The second step involves the design of the feedforward controllers, for which a perfect preview is assumed. Several controller proposals based on a sequential approach can be found in the literature [3,4].

Although the decoupling in two steps might account for a simpler design of the controller, it might also lead to a sub-optimal design. Therefore, a second group of design methodologies is based on a single step design in which the measurement error is taken into account. These robust control design techniques, which have been specially developed to deal with errors and uncertainties, provide an interesting tool for the design of LIDAR assisted controllers. Thus, by including uncertain models during the design of the controllers, a real-case optimal operation can be achieved.

The standard way to represent the realistic measurement of a LIDAR sensor is using a frequency response function that represents its nominal behaviour and a coherence function as a measure of the non-linearity between measured and rotor effective wind speed. This frequency domain representation seems adequate, as wind is defined theoretically in the frequency domain and many controllers are designed in the frequency domain as well. Additionally, although it is not possible to develop analytical models of LIDAR sensors providing realistic representations of all the different sources of error [5], frequency domain identification provides a well-known, straightforward way to obtain realistic models from measured data.

Even though the model formed by the frequency response data and the coherence function has been used for determining the best sensor configuration [6,7] and in some optimization-based designs [8], it is not suitable for every robust design methodology. More specifically, the tools used for the design of μ-synthesis and QFT (Quantitative Feedback Theory) controllers require uncertain systems to be modelled as a set of linear time invariant (LTI) systems. These uncertain models can either have a fixed structure with unknown parameters (parametric uncertainty) or have some nominal response and a bound to the possible deviation around it (non-parametric uncertainty).

* Corresponding author.
E-mail address: irene.miquelez@unavarra.es (I. Miquelez-Madariaga).

https://doi.org/10.1016/j.renene.2023.02.062
Received 3 July 2022; Received in revised form 11 February 2023; Accepted 14 February 2023
Available online 16 February 2023

Nomenclature

$\beta(t)$	Pitch angle demand
$\gamma^2_{xy}(t)$	Squared coherence function of signals $x(t)$ and $y(t)$
$\Omega_g(t)$	Generator speed
θ	Angular direction in the rotor plane coordinate system
φ	Random phase in the uncertain model $H(s,\varphi)$
c_P	Power coefficient
$C_{FB}(s)$	Feedback controller
$F(s)$	Feedforward controller
$G_{y,x}(s)$	Transfer functions of the wind turbine model
$H(s,\varphi)$	Linear uncertain LIDAR model
$h_0(t)$	Impulse response of the linearized system
$n(t)$	Random noise of a generic nonlinear process
r	Radial direction in the rotor plane coordinate system
$R_{xx}(t)$	Auto-correlation of signal $x(t)$
$R_{yx}(t)$	Cross-correlation between signals $x(t)$ and $y(t)$
$S_{xx}(\omega)$	Power spectrum of signal $x(t)$
$S_{yx}(\omega)$	Cross power spectrum of signals $x(t)$ and $y(t)$
$T_{y,x}(s)$	Closed loop transfer function
w_{field}	Turbulent 4-dimensional wind field
$w_L(t)$	Measured wind speed
$w_R(t)$	Rotor effective wind speed
$w_u(t)$	Wind speed perpendicular to the rotor plane
WTG	Realistic nonlinear wind turbine model
$x(t)$	Random input of a generic nonlinear process
$y(t)$	Random output of a generic nonlinear process

The main contribution of this work is the novel theoretical relation between measurement noise and model uncertainty developed in Section 3. Experts on LIDAR sensors and wind measurement use the estimated noise signal and coherence function to model the non-linearities of the measurement process. However, the most well-known robust control design methodologies, such as mu synthesis and QFT, work best when the non-linearities are represented by means of model uncertainty instead of a noise signal. Generally speaking, the main contribution of this paper allows to obtain uncertain models directly from the data obtained by identification (measured signal spectra and coherence function). More specifically, in the context of LIDAR assisted control, it allows transforming the valuable experimental models of the LIDAR sensor into uncertain models, which contain the same information but allow to use multi-objective and robust controller design methodologies.

The structure of this work is as follows. Section 2 introduces a brief review on frequency domain identification of linear systems and Section 3 provides a theoretical relation between the traditional coherence model and a LTI uncertain model required for robust control design. Section 4 describes the different components needed for a realistic simulation of a nacelle-mounted LIDAR sensor: a wind turbine, its control loops, a wind field vector and the LIDAR sensor itself. The LTI uncertain model of the mentioned LIDAR sensor is validated on Section 5. Section 6 contains the conclusions of the work.

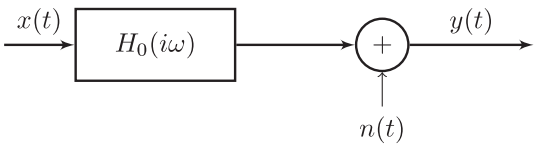

Fig. 1. Block diagram of a linear system with noise at the output.

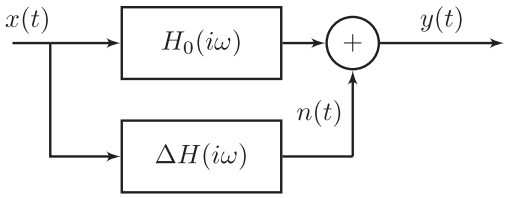

Fig. 2. System with additive uncertainty.

2. Review of frequency domain identification of linear models

Obtaining mathematical models that describe the behaviour of physical systems is a common problem in many engineering fields. More specifically, when designing controllers, it is necessary to have a model of the relation between the input signals of the system, either control input or disturbance, and the outputs to be controlled.

If small variations in the input are assumed, the behaviour of a single-input–single-output system can be approximated to a linear one [9], which follows the structure represented in Fig. 1. In order to find the value of $H_0(i\omega)$, $x(t)$ and $y(t)$ need to be measured. The noise input $n(t)$, is linearly independent of $x(t)$ and represents the effect of other inputs in $y(t)$, the nonlinear relation between $x(t)$ and $y(t)$, and measurement noise.

The relation between the signals represented in Fig. 1 can be expressed mathematically as

$$y(t) = \int_0^t h_0(u)x(t-u)du + n(t), \tag{1}$$

where $h_0(u)$ is the impulse response of the linear system. Multiplying both sides of the equation by $x(t-\tau)$ we obtain

$$y(t)x(t-\tau) = \int_0^t h_0(u)x(t-\tau)x(t-u)du + n(t)x(t-\tau), \tag{2}$$

whose expected value is

$$R_{xy}(\tau) = \int_0^t h_0(u)R_{xx}(\tau-u)du, \tag{3}$$

where $R_{xy}(\tau)$ is the cross correlation between $x(t)$ and $y(t)$ and $R_{xx}(\tau)$ is the auto-correlation of signal $x(t)$. The term including the noise signal $n(t)$ disappears because the noise is linearly independent from the input and, consequently, their cross correlation is equal to zero.

Applying the Fourier transform to both sides of Eq. (3), the convolution between the system's impulse response and the auto-correlation of the input becomes a multiplication, and the correlation functions become power spectral densities, as given by

$$S_{xy}(\omega) = H_0(i\omega)S_{xx}(\omega). \tag{4}$$

Consequently, if the power spectral density of the input $S_{xx}(\omega)$ and the cross power spectral density of the input and the output $S_{xy}(\omega)$ can be calculated from measurements of $x(t)$ and $y(t)$, it is possible to obtain the transfer function $H_0(i\omega)$.

As the noise signal $n(t)$ is not a real signal within the system, but a mathematical representation of non-linearities and other effects, it is

not possible to measure it. However, as explained by Ljung [10], its power spectrum can be derived from the power spectral densities of the input and output signals:

$$S_{nn}(\omega) = S_{yy}(\omega) - |H_0(\omega)|^2 S_{xx}(\omega) = S_{yy}(\omega) - \frac{|S_{xy}(\omega)|^2}{S_{xx}(\omega)}. \tag{5}$$

As it happens with the cross correlation, the cross spectral density function is bounded by the cross spectral density inequality [11] given by

$$|S_{xy}(\omega)|^2 \leq |S_{yy}(\omega)|\,|S_{xx}(\omega)|. \tag{6}$$

The square coherence function is defined as a normalized expression of the cross power spectral density:

$$\gamma_{xy}^2(\omega) = \frac{|S_{xy}(\omega)|^2}{S_{yy}(\omega)S_{xx}(\omega)}. \tag{7}$$

The coherence function is defined for all ω for which $S_{xx}(\omega)$ and $S_{yy}(\omega)$ are defined. Being a normalized function, it fulfils

$$0 \leq \gamma_{xy}^2(\omega) \leq 1. \tag{8}$$

Using Eq. (5), the coherence function can be also expressed as

$$\gamma_{xy}^2(\omega) = \frac{|H_0(i\omega)|^2 S_{xx}(\omega)}{S_{nn}(\omega) + |H_0(i\omega)|^2 S_{xx}(\omega)} = \frac{|H_0(i\omega)|^2 S_{xx}(\omega)}{S_{yy}(\omega)}. \tag{9}$$

In other words, the squared coherence represents the fraction of the power in the output that is linearly dependent from the input $x(t)$. Consequently, if the original system is linear, it will be completely represented by $H_0(i\omega)$, $n(t)$ will be equal to 0 and the squared coherence will be equal to 1. If $x(t)$ and $y(t)$ are linearly independent, $\gamma_{xy}^2(\omega)$ will be equal to 0.

Using Eqs. (5) and (9), the noise spectrum can be written in terms of the squared coherence as

$$S_{nn}(\omega) = S_{yy}(\omega)(1 - \gamma_{xy}^2(\omega)). \tag{10}$$

When generating a model for a LIDAR sensor, signal $x(t)$ will be rotor effective wind speed (defined in Section, Eq. (15)), signal $y(t)$ will be the actual measured wind signal and $n(t)$ will be the measurement noise.

3. Theoretical relation between the coherence function and additive uncertainty

The purpose of this section is to set a theoretical relation between the linear model of a system defined by Eqs. (4) and (10) (Fig. 1), and a uncertain LTI system (Fig. 2). In terms of LIDAR assisted control, the model in Fig. 1 is often generated using data from field measurements or a realistic non-linear simulation. The model in Fig. 2 is better suited fro controller design and is compatible with Matlab's *Robust Control Toolbox* and the *QFT toolbox*.

Although coherence is clearly related to the systems uncertainty caused by both the unmodelled dynamics and the uncertain parameters, it might not be a suitable representation of the uncertainty for control purposes. For some design methodologies, such as H_∞ or QFT, robust stability and performance are imposed on a set of possible linear time invariant plants, known as the uncertainty set, which captures the nonlinear behaviour of the system and other sources of uncertainty [12].

There exist several ways to express uncertainty. If the frequency response of the uncertain set $H(i\omega, q)$ is represented in the complex plane at a single frequency ω_0, it is common to have a nominal system represented by the complex number $H_0(i\omega_0)$ and a region around it, usually a circle, representing the set of possible values for such number. These circular bounds can be expressed mathematically in different ways [13], such as additive uncertainty, in which an uncertain system is described as

$$H(i\omega) = H_0(i\omega) + \Delta H(i\omega), \tag{11}$$

and $\Delta H(i\omega)$ is some bounded value.

Fig. 2 shows a graphical representation of a linear system with additive uncertainty. By comparing this system to the one represented in Fig. 1, a relation between signals $x(t)$ and $n(t)$ can be established by the uncertainty block $\Delta H(i\omega)$. This new perspective implies that the external noise sources in Fig. 1 are the uncertainty sources embedded in the linear model in Fig. 2.

However, as the cross spectrum between $x(t)$ and $n(t)$ cannot be estimated, only the magnitude of the uncertainty is known, as given by

$$|\Delta H(i\omega)|^2 = \frac{S_{nn}(\omega)}{S_{xx}(\omega)}. \tag{12}$$

In this case, the magnitude of $\Delta H(i\omega)$ is fixed by the amplitude of the noise and the uncertainty comes only in the phase. Consequently, if the uncertain system is represented at a single frequency in the complex plane, it will take the form of a circle with centre in $H_0(i\omega)$ and radius $|\Delta H(i\omega)|$, which means

$$H(i\omega, \varphi) = H_0(i\omega) + |\Delta H(i\omega)|e^{i\varphi}, \tag{13}$$

where φ randomly takes any value between 0 and 2π.

Seeing that the size of the uncertain system is related to the magnitude of the noise signal power spectral density, a further step is taken to link the uncertain model with the coherence function. This way a connection appears between the usual indicator of measurement quality and a control-oriented representation of the systems uncertainty. Using Eqs. (9), (10) and (12), the relation between the coherence function and the size of uncertainty becomes

$$\frac{|\Delta H(i\omega)|}{|H_0(i\omega)|} = \sqrt{\frac{1 - \gamma_{xy}^2(\omega)}{\gamma_{xy}^2(\omega)}}. \tag{14}$$

This equation confirms the expected result between models: a perfect coherence ($\gamma_{xy}^2(\omega) = 1$) leads to an uncertainty-free model ($\Delta H(i\omega) = 0$), whereas a coherence value of zero ($\gamma_{xy}^2(\omega) = 0$) implies infinite uncertainty ($\Delta H(i\omega) = \infty$).

The objective of representing a nonlinear system as a set of linear models is thus achieved, as there exists an analytical relation between the coherence function and the size of the uncertainty in the frequency response function of the system.

4. A realistic nonlinear simulator of a LIDAR sensor

In order to validate the proposed linear approximation of a nonlinear system, the outputs of nonlinear simulations are compared with their linear approximations. More specifically, a nacelle-mounted LIDAR sensor is approximated by an uncertain linear system which can later on be used for control design purposes. However, this model cannot be tested on its own, as many of the measurement errors are induced by the coupling between the sensor and the wind turbine it is installed on, blade-crossing and the tower fore-aft movement among others. As a consequence, the linear model of the LIDAR model is used, together with the linear model of a wind turbine and its control loops, to predict the output of a nonlinear simulation of a wind turbine operating with a LIDAR-based feedforward controller. The chosen aeroelastic code for this simulation is OpenFAST [14], as it includes both the wind turbine and the LIDAR module, which was validated using field data [15]. This section describes all the elements involved in the simulations.

4.1. LIDAR sensor

The chosen LIDAR system has a 4 beam configuration. The azimuth angles of the beams are ±15° and the elevation angles are ±12.5°. The measurement distance of the beams is 85 m and the pulse width at half maximum is 30 m and a full scan takes 1 s.

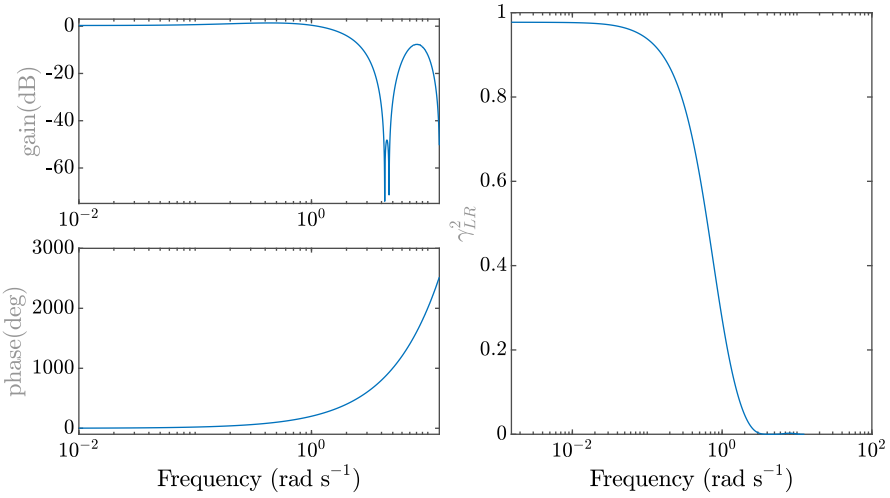

Fig. 3. (a) Frequency response of the LIDAR system at the operation point corresponding to a wind speed of 20 m s^{-1}. (b) Coherence function of the LIDAR system.

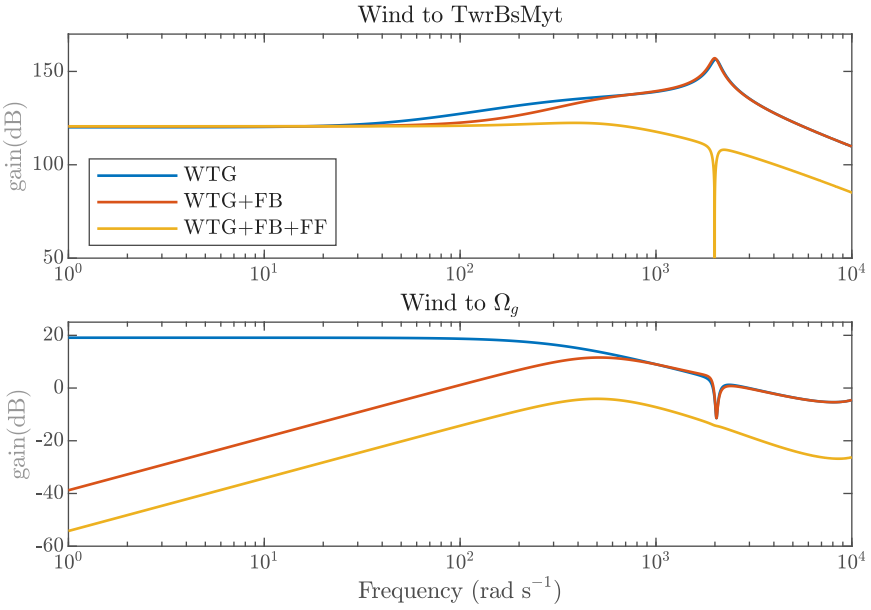

Fig. 4. Frequency response of the wind turbine (WTG), the wind turbine in closed loop operation (WTG+FB) and the wind turbine with both feedback and feedforward control loops (WTG+FB+FF). The input to the system is the wind speed and the studied outputs are tower base bending moment (TwrBsMyt) and generator speed (GenSpeed).

Due to the limited measurement capability of the sensor, both in terms of sampling frequency and spatial distribution, and other effects described in the bibliography, such as the wind field evolution or the coupling of the beams with the wind turbine blades, the LIDAR system cannot be considered to have a linear behaviour, which means that the measured signal includes some measurement noise.

For many wind turbine applications, it is enough to get information on the average wind on the rotor plane, also known as rotor effective wind speed (REWS). As a consequence, rotor effective wind speed will be considered the input to the linear model of the sensor. Theoretically, REWS is given by

$$w_R(t) = \sqrt[3]{\frac{\int_0^{2\pi}\int_0^R w_u^3(r,\theta,t)\frac{\partial c_P}{\partial r}drd\theta}{\int_0^{2\pi}\int_0^R \frac{\partial c_P}{\partial r}drd\theta}}, \tag{15}$$

where w_u is the wind speed in the direction perpendicular to the rotor, r and θ are the polar coordinates in the rotor plane, and c_P is the power coefficient of the wind turbine. The spectrum of such signal $S_{RR}(\omega)$ is related to the spectrum of the measured wind signal $S_{LL}(\omega)$ by means of the frequency response function of the sensor $H_0(i\omega)$ (Fig. 3a) following Eq. (4), where $S_{RR}(\omega)$ and $S_{LL}(\omega)$ are now the spectra of the input and the output of the system respectively. Fig. 3b shows the coherence function $\gamma^2_{LR}(\omega)$ between the signals as given by Eq. (7).

4.2. Wind turbine generator

The wind turbine used for this study is the onshore 5 MW NREL model [16], which is a horizontal axis, three-bladed turbine. For a realistic representation of the behaviour of a wind turbine, all degrees of freedom except the rotor teeter are activated both during the simulation and the linearization of the system. The most relevant parameters of the wind turbine are presented in Table 1.

4.3. Control structures

The linear model is validated at above rated operation of the wind turbine, using a constant torque strategy. Consequently, the wind turbine requires a collective pitch feedback controller, given by

$$C_{FB}(s) = \frac{0.003383s + 0.001865}{s}, \tag{16}$$

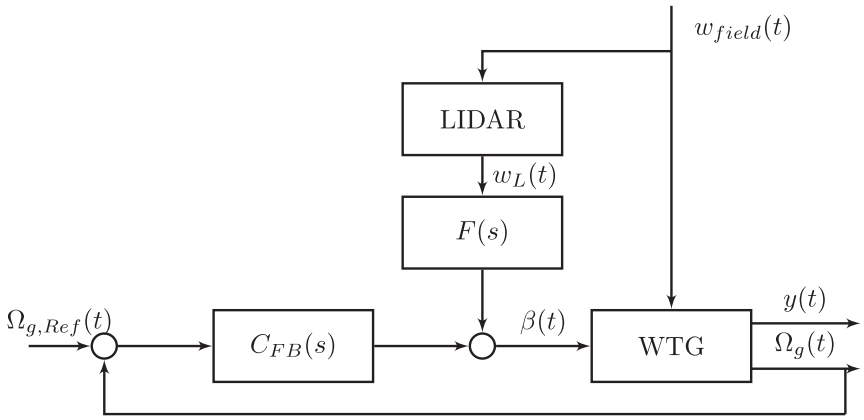

Fig. 5. Block diagram of the nonlinear simulation scenario.

Table 1
Parameters for the 5 MW NREL wind turbine [16].

Parameter	Value
Rotor diameter	126 m
Hub height	90 m
Cut-in rotor speed	6.9 rpm
Rated rotor speed	12.1 rpm

that ensures a correct generator speed regulation.

Besides, to see the effect of the measurement error in the output, a collective pitch feedforward controller given by

$$F(s) = \frac{0.009436s + 0.01784}{0.4754s + 1} \tag{17}$$

is added. The feedforward controller has a simple first order structure with one zero and its parameters are chosen to obtain perfect model inversion at a single frequency [17].

Fig. 4 shows the open loop response of the system, the effect of the feedback controller and the addition of the feedforward controller, assuming perfect preview.

5. Validation of the model using simulation data

The theoretical relation between the coherence and the size of the uncertainty of the frequency response function, shown in Eq. (14), is validated using simulation data. For the new model to be correct, it should provide the same information as the model that represents the measured wind as an input independent from the rotor effective wind speed (Fig. 6a). At the same time, it should be an accurate approximation of the nonlinear system (Fig. 5).

To carry out the analysis, a turbulent wind field of mean wind speed of 20 m s^{-1}, class A and length 4096 s generated with Turbsim [18] has been simulated in the system represented in Fig. 5. The analysis could have been performed at any other wind speed at the above rated operation region without losing its validity, but for the sake of simplicity, it has been developed at a single mean wind speed. Besides, using simulations with different mean speeds for the same analysis, for example 19 to 21 m s^{-1} instead of just 20 m s^{-1}, would provide a model valid at a wider range or wind speeds but would also increase the uncertainty introduced by the linearization. Lastly, one must take into account that, as the linear models are tested under the turbulent wind fields corresponding to the wind turbine class, the new linear model has been tested against the traditional linear representation and the nonlinear system in a realistic environment. This means that the nonlinear system undergoes as sudden wind speed changes as one can expect in normal operation. Extreme gusts not represented by this turbulent wind model would require a specific analysis and design.

The block WTG represents the nonlinear model of the wind turbine, the block LIDAR represents the realistic LIDAR simulator and blocks $C_{FB}(s)$ and $F(s)$ represent the feedback and feedforward controllers. Output signals generator speed (GenSpeed) and longitudinal tower base bending moment (TwrBsMyt) are used for the validation. Their spectra are represented in Fig. 8 by the line $FF - OpenFAST$.

Fig. 6a shows the common representation of the linear model of the system. Now, the wind turbine is described by its linearized model $G_{WTG}(s)$, whose input is no longer a wind field but the rotor effective wind speed $W_R(s)$. The LIDAR system is represented by a second wind input, the measured wind $W_L(s)$, whose relation to $W_R(s)$ is described by the frequency response and the coherence functions shown in Fig. 3.

According to this lineal modelling, a generic output $Y(s)$ is given by

$$\begin{aligned} Y_{\gamma^2}(s) &= \frac{G_{y,W_R}(s)}{1 + C_{FB}(s) \cdot G_{\Omega_g,\beta}(s)} W_R(s) + \frac{F(s) \cdot G_{y,\beta}(s)}{1 + C_{FB}(s) \cdot G_{\Omega_g,\beta}(s)} W_L(s) \\ &= T_{y,W_R}(s) W_R(s) + T_{y,W_L}(s) W_L(s) \end{aligned} \tag{18}$$

where $G_{y,u}(s)$ and $T_{y,u}(s)$ denote the open loop and closed loop transfer functions of the wind turbine between any input $U(s)$ (typically wind, pitch or generator torque) and any output $Y(s)$, such as the generator speed or any mechanical load among others. More specifically, Ω_g stands for the generator speed signal and β represents the collective pitch angle demand.

A theoretical approximation of the power spectra of outputs of the system can be obtained from Eq. (18) as

$$\begin{aligned} S_{yy,\gamma^2}(\omega) = &|T_{y,W_R}(i\omega)|^2 S_{RR}(\omega) \\ &+ T_{y,W_R}(i\omega) T^*_{y,W_L}(i\omega) S_{RL}(\omega) \\ &+ T^*_{y,W_R}(i\omega) T_{y,W_L}(i\omega) S_{LR}(\omega) \\ &+ |T_{y,W_L}(i\omega)|^2 S_{LL}(\omega) \end{aligned} \tag{19}$$

The results have been represented in Fig. 8 by the lines $FF - \gamma^2$ and are almost overlapped with the simulation output spectra ($FF - OpenFAST$), thus showing a very good correspondence between nonlinear and linear models.

If correct, the alternative model developed in this work (Fig. 6b) should provide the same results as the previous ones. The sensor is now represented by a set of linear time invariant models, $H(s, \varphi)$ in Fig. 7, with input rotor effective wind speed and output measured wind. The nominal system $H_0(s)$ corresponds to the frequency response data in Fig. 3 and the size of its uncertainty $\Delta H(s)$ has been obtained by applying Eq. (14). The complete closed loop system has now a single input, rotor effective wind speed, and a set of possible outputs $Y(s, \varphi)$

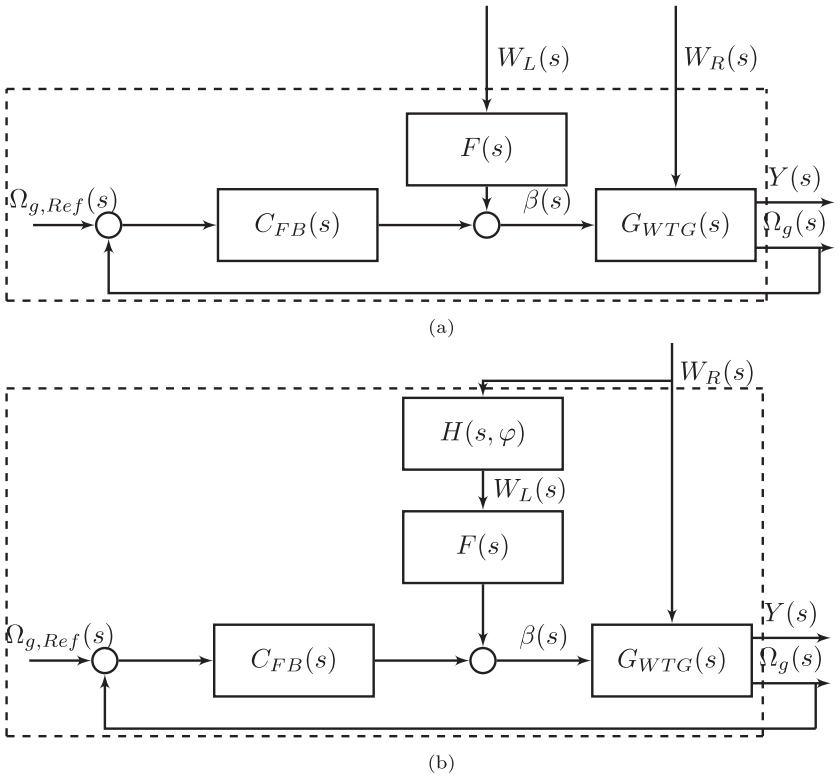

Fig. 6. Linear representations of the model in Fig. 5. Block diagram *a* uses a signal $W_L(s)$ to represent the measured wind. Block diagram *b* represents the LIDAR sensor as an uncertain system $H(s,\varphi)$.

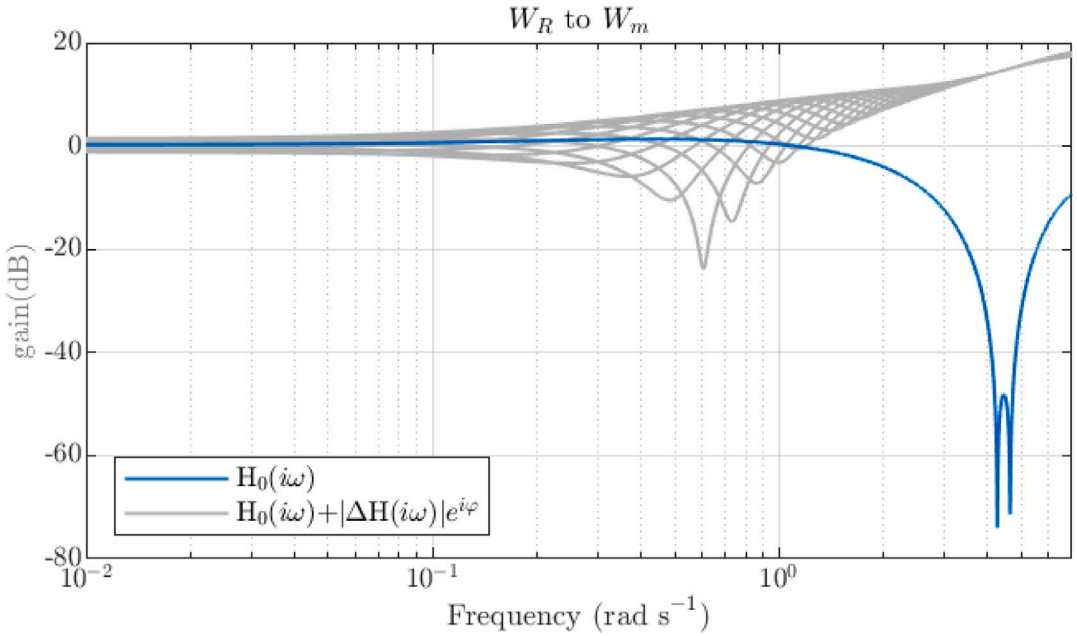

Fig. 7. Magnitude plot of the frequency response of the LIDAR system. In blue, the nominal response of the system $H_0(\omega)$. In grey, the outer bound of the uncertain system given by $H(i\omega,\varphi) = H_0(i\omega) + |\Delta H(i\omega)|e^{i\varphi}$.

is given by

$$Y_{\Delta H}(s,\varphi) = \frac{G_{y,W_R}(s) + F(s)\cdot H(s,\varphi)\cdot G_{y,\beta}(s)}{1 + C_{FB}(s)\cdot G_{\Omega_g,\beta}(s)} W_R(s) = T'_{y,W_R}(s,\varphi) W_R(s), \tag{20}$$

where $T'_{y,W_R}(s,\varphi)$ now includes the LIDAR linear model and the feed-forward controller.

The set of possible output spectra is

$$S_{yy,\Delta H}(\omega,\varphi) = |T'_{y,W_R}(i\omega,\varphi)|^2 S_{RR}(\omega), \tag{21}$$

which is represented by the set of lines $FF - \Delta H(i\omega,\varphi)$ in Fig. 8. The average behaviour of the system is defined by the average of these spectra which is represented by $FF - \Delta H(i\omega)$. As anticipated by the theoretical relation developed in Section 3, the information provided using the new linear approximation is just the same as the model that

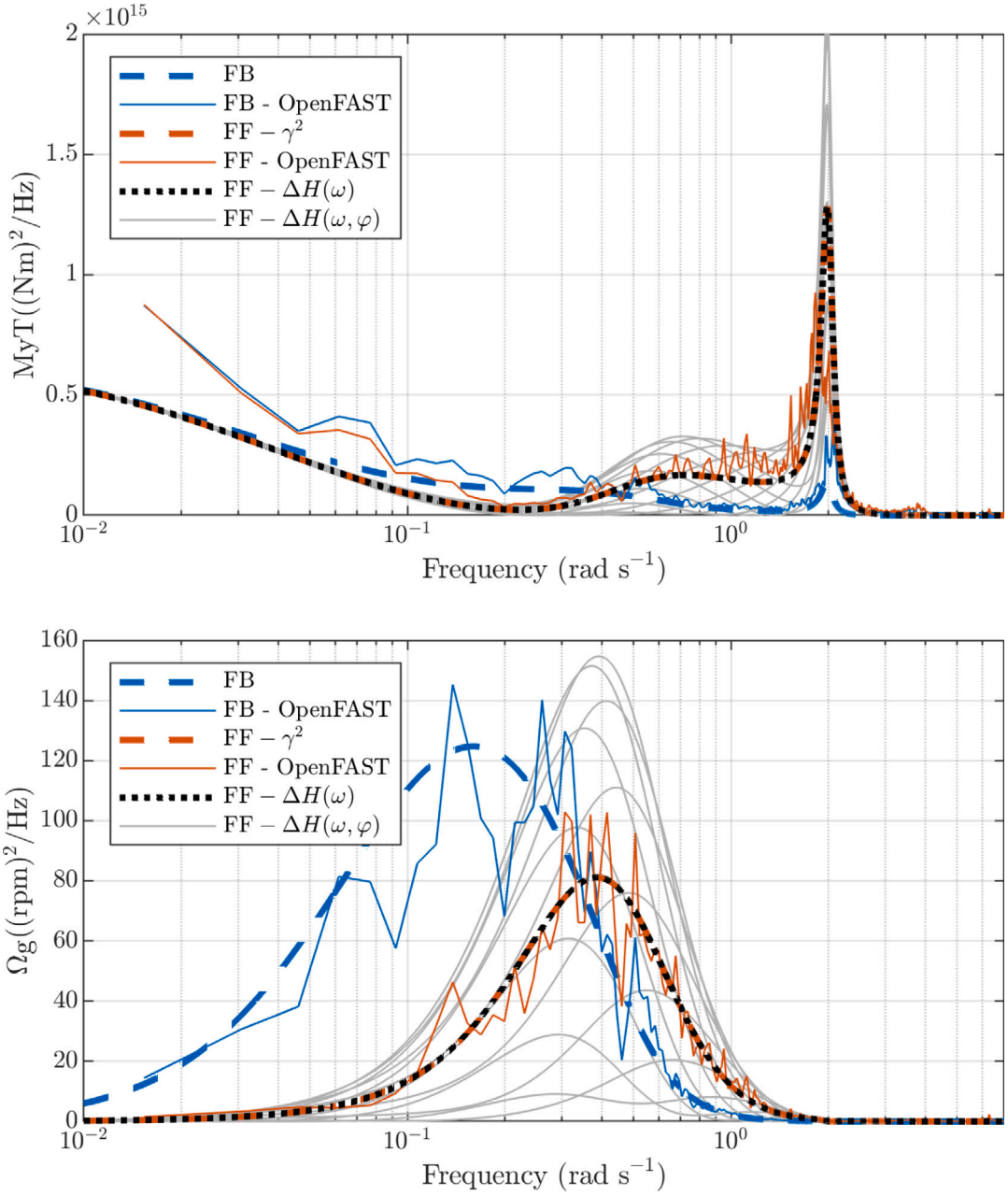

Fig. 8. Spectra of the output signals. The lines denoted with OpenFAST correspond to the spectra estimated from simulation of the feedback only case (blue) and feedback + feedforward control (red). The dashed blue line represents the theoretical spectrum of the feedback only case. The red dashed line (FF-γ^2) is the theoretical spectrum of the output using the coherence function to represent the error in the measurement. The grey lines (FF-$\Delta H(\omega, \varphi)$) correspond to all the possible responses of the closed loop linear system representing the LIDAR sensor as a uncertain linear system with a single input. Their frequency domain average is represented by the dashed black line (FF-$\Delta H(\omega)$).

considers the coherence function and can be thus considered valid for robust controller design purposes.

6. Conclusions

This paper presents a theoretical relation between the coherence based model of the measurement noise introduced by a LIDAR sensor and a non-parametric uncertain linear model. The relation between the coherence function $\gamma^2_{xy}(\omega)$ and the size of the non-parametric uncertainty $|\Delta H(i\omega)|$ shows two different ways of representing the same information: a linear approximation of the behaviour of a nonlinear system and the degree of its non-linearity.

The difference between models is relevant when using linear systems to design controllers. The coherence-based model has two inputs and produces a single output that represents the average behaviour of the system. On the other hand, the uncertain system described by $H_0(i\omega)+|\Delta H(i\omega)|$ has a single input but, as it represents the uncertainty, it provides the set of all the possible outputs of the actual system. One model being more adequate than the other would depend on the intended purpose for it. However, when applying robust control methodologies such as H∞ design or QFT, the uncertainty set $H(s, \varphi)$ will be preferred, as it allows to use typical design criteria such as robust stability and performance, and it makes it easier to evaluate multiple control objectives simultaneously.

CRediT authorship contribution statement

Irene Miquelez-Madariaga: Conceptualization, Methodology, Writing. **Idoia Lizarraga-Zubéldia:** Software, Validation. **Asier Diaz**

de Corcuera: Funding, Supervision, Writing – reviewing. **Jorge Elso:** Conceptualization, Methodology, Writing – reviewing.

Declaration of competing interest

The authors declare that they have no known competing financial interests or personal relationships that could have appeared to influence the work reported in this paper.

Acknowledgements

The authors gratefully appreciate the support given by Siemens Gamesa Renewable Energy, Spain through the predoctoral research contract no. 1055/2020. Open access funding provided by Universidad Pública de Navarra.

References

[1] E. Simley, H. Fürst, F. Haizmann, D. Schlipf, Optimizing lidars for wind turbine control applications—Results from the IEA wind task 32 workshop, Remote Sens. 10 (6) (2018) 863.

[2] D. Schlipf, H. Fürst, S. Raach, F. Haizmann, Systems engineering for Lidar-assisted control: A sequential approach, in: Journal of Physics: Conference Series, Vol. 1102,1, IOP Publishing, 2018, 012014.

[3] F. Dunne, L. Pao, A. Wright, B. Jonkman, N. Kelley, E. Simley, Adding feedforward blade pitch control for load mitigation in wind turbines: Non-causal series expansion, preview control, and optimized FIR filter methods, in: 49th AIAA Aerospace Sciences Meeting including the New Horizons Forum and Aerospace Exposition, 2011, http://dx.doi.org/10.2514/6.2011-819.

[4] N. Wang, K.E. Johnson, A.D. Wright, LIDAR-based FX-RLS feedforward control for wind turbine load mitigation, in: Proceedings of the 2011 American Control Conference, IEEE, 2011, pp. 1910–1915.

[5] D. Schlipf, P.W. Cheng, J. Mann, Model of the correlation between lidar systems and wind turbines for lidar-assisted control, J. Atmos. Ocean. Technol. 30 (10) (2013) 2233–2240.

[6] F. Dunne, L.Y. Pao, D. Schlipf, A.K. Scholbrock, Importance of lidar measurement timing accuracy for wind turbine control, in: 2014 American Control Conference, IEEE, 2014, pp. 3716–3721.

[7] R. Ungurán, V. Petrović, L.Y. Pao, M. Kühn, Uncertainty identification of blade-mounted lidar-based inflow wind speed measurements for robust feedback–feedforward control synthesis, Wind Energy Sci. 4 (4) (2019) 677–692.

[8] F. Dunne, L.Y. Pao, Benefit of wind turbine preview control as a function of measurement coherence and preview time, in: 2013 American Control Conference, IEEE, 2013, pp. 647–652.

[9] G. Jenkins, An example of the estimation of a linear open loop transfer function, Technometrics 5 (2) (1963) 227–245.

[10] L. Ljung, et al., Theory for the user, in: System Identification, Prentice-hall, Inc., 1987.

[11] J.S. Bendat, A.G. Piersol, Random Data: Analysis and Measurement Procedures, vol. 729, John Wiley & Sons, 2011.

[12] S. Skogestad, I. Postlethwaite, Multivariable Feedback Control: Analysis and Design, vol. 2, Citeseer, 2007.

[13] S.G. Douma, P.M. Van den Hof, Relations between uncertainty structures in identification for robust control, Automatica 41 (3) (2005) 439–457.

[14] Open-source wind turbine simulation tool, OpenFAST, http://github.com/OpenFAST/OpenFAST/.

[15] F. Guo, D. Schlipf, H. Zhu, A. Platt, P.W. Cheng, F. Thomas, Updates on the openfast lidar simulator, J. Phys. Conf. Ser. 2265 (4) (2022) 042030, http://dx.doi.org/10.1088/1742-6596/2265/4/042030.

[16] J. Jonkman, S. Butterfield, W. Musial, G. Scott, Definition of a 5-MW Reference Wind Turbine for Offshore System Development, Tech. rep., National Renewable Energy Lab.(NREL), Golden, CO (United States), 2009.

[17] I. Miquelez-Madariaga, I. Lizarraga-Zubeldia, A. Diaz-de Corcuera, J. Elso, Lidar-based feedforward control design methodology for tower load alleviation in wind turbines, Wind Energy (2022).

[18] B. Jonkman, M. Buhl Jr., Turbsim User's Guide, Tech. rep., National Renewable Energy Lab.(NREL), Golden, CO (United States), 2006.